Scientific article
UDC 546.881.3:54.03
DOI: 10.52957/2782-1900-2026-7-2-131-142

MECHANOCHEMICAL TREATMENT OF SHOT-BLASTING CLEANING PRODUCTS OF V–AL MASTER ALLOY INGOTS FOR SYNTHESIS OF AL-BASED COMPOSITES

M.N. Baklanov[1*], D.A. Eselevich[1], V.G. Shevchenko[1], S.V. Kobyakov[2], N.A. Popov[1]

Maxim Nikolaevich Baklanov; Danil Aleksandrovich Eselevich, Candidate of Chemical Sciences; **Vladimir Grigorievich Shevchenko,** Doctor of Chemical Sciences; **Stanislav Vadimovich Kobyakov; Nikolai Alexandrovich Popov,** Candidate of Chemical Sciences

[1]Institute of Solid State Chemistry, Ural Branch of the Russian Academy of Sciences, 91 Pervomayskaya St., Yekaterinburg, 620077, Russia;

[2]Ural Federal University named after B.N. Yeltsin, 19 Ulitsa Mira, Yekaterinburg, 620062, Russia.

baklanov_mn@vsmpo-avisma.ru, diablohulk@gmail.com, shevchenko@ihim.uran.ru, pipupgradepip@mail.ru, n168@mail.ru

Keywords: *aluminum, amorphization, shot-blasting dust, dispersion-strengthened composite, reactivity*

Abstract. *The paper demonstrates an effective possibility of using waste (shot-blasting dust) from the production of V–Al master alloys for obtaining the dispersion-strengthened composite materials based on aluminum. An analysis of the chemical, phase, and granulometric composition of dust from VnAl-65 and VnAl-1 master alloys has been conducted. To increase the reactivity, the shot-blasting dust (SBD) was subjected to mechanical activation in a planetary mill with the establishment of the optimal processing time. It significantly reduces the average particle size up to 8 μm with an increase in specific surface area by several times and induces amorphization of* Al_2O_3*. According to XRD analysis and electron microscopy, during the sintering of mixtures (Al +* $SBD_{VnAl\text{-}65}$*, Al +* $SBD_{VnAl\text{-}1}$*), a composite material is formed. Moreover, strengthening intermetallic compounds (*Al_3V*,* $Al_{23}V_4$ *and* Fe_4Al_{13}*) are uniformly distributed in the aluminum matrix – a solid solution of V in Al.*

For citation:
Baklanov M.N., Eselevich D.A., Shevchenko V.G., Kobyakov S.V., Popov N.A. Mechanochemical treatment of shot-blasting cleaning products of V–Al master alloy ingots for synthesis of Al-based composites // From Chemistry towards Technology Step-by-Step. 2026. Vol. 7, Iss. 2. P. 131-142. URL: https://chemintech.ru/en/nauka/issue/7273/view

Introduction

During the production of master alloys for titanium alloys at JSC "Uralredmet" (the Sverdlovsk region, Verhnyaya Pishma, The Russian Federation) there is generation and accumulation of disperse dust after filtration in the ventilation system of shot-blasting units.

Those are in use in the manufacture of components for the aerospace industry, defense equipment, shipbuilding, and chemical engineering [1]. The products of shot-blasting cleaning of master alloys are not further utilized and recycled. Due to the absence of comprehensive technologies for their processing for subsequent reintroduction into production and the lack of capabilities for enterprises to master more advanced reprocessing stages, this industrial by-product does not find wide application at domestic metallurgical enterprises [2].

On the one hand, the processing of disperse industrial by-products and their remelting are complex technological stages in the involvement of waste in the production of high-quality master alloys, alloys, and special additives. It is complicated by the variable composition and metallurgical properties of the dust, its explosion, and fire hazard. It also applies to the processing of disperse material from the filter unit after cleaning master alloy ingots of various compositions in shot-blasting machines at JSC "Uralredmet".

On the other hand, the products of processing master alloy ingots (V, Mo, Ti with Al) could be applied in the manufacture of new composite alloys and materials due to the rather high content of intermetallic compounds. For example, in [3], a composite alloy of the Al–V system was obtained; aluminum acts as the matrix and the intermetallic compound Al_3V acts as the reinforcing component.

The initial state of the powder mixture is important for controlling the processes of reactive sintering of the components of the Al–V system. Mechanical activation through the processing of powders in high-energy attritors is a method of intensifying technological processes for obtaining materials [4, 5]. During this process, a reduction in particle size and an increase in their specific surface area occur, along with mixing and accumulation of structural defects in the crystal lattice, and the formation of chemical compounds. For example, it occurs in the synthesis of a composite material based on an aluminum–vanadium alloy [6]. In [7], the efficiency of mechanical activation depends on the type of mill, the energy intensity of the process, and the processing time. For example, excessive grinding can lead to welding of particles and the formation of difficult-to-separate agglomerates (the mechanic-welding effect) [5]. Therefore, the search for optimal grinding conditions will contribute to the efficiency of the subsequent synthesis of the functional material.

Current trends in the global metallurgical industry demonstrate a shift toward sustainable development and the circular economy. Indeed, the processing of technogenic waste is becoming one of the most important tasks for preserving the resource base and reducing environmental impact [8]. For example, PJSC MMC Norilsk Nickel (The Russian Federation), successfully implemented the projects for the recycling of tailings from metallurgical production. It confirms the effectiveness of incorporating secondary raw materials into economic circulation [9].

Our previous studies [10] confirmed the fundamental feasibility of using shot-blasting dust from the V–Al master alloy as a feedstock for obtaining an aluminum-matrix composite. However, to optimize the composition and structure of the final materials, a detailed investigation of fractional composition of shot-blasting dust influence (SBD), mechanical activation conditions, and heat treatment is required.

The purpose of this study is to optimize the method of using disperse waste (shot-blasting dust) generated during the production of V–Al master alloys for obtaining aluminum-based composite materials with high functional properties. The objectives of the study are: analysis of the chemical, phase, and granulometric composition of shot-blasting dust from VnAl-1 and VnAl-65 master alloys; investigation of the effect of mechanical activation (grinding in a planetary mill) on the morphology, dispersity, and phase composition of dust particles; optimization of the synthesis method for new composite materials using shot-blasting dust, and elucidation of the strengthening mechanisms of the aluminum matrix during sintering.

Methods of investigation and sample preparation

For the study, shot-blasting dust from master alloys of grades VnAl-65 with a high vanadium content (65 wt. %) and VnAl-1 (V – 70 wt. %) was used.

The phase composition of the samples (initial SBD and synthesized composites) was investigated using a STADI-P powder X-ray diffractometer (STOE, Germany) with $CuK\alpha_1$ radiation, using the PDF-2 X-ray diffraction data library (Release 2009). Quantitative phase analysis was performed by the Rietveld method using the MAUD (Material Analysis Using Diffraction) software [11]. To study the surface morphology of powder mixture particles and sintered materials, an analytical scanning electron microscope TESCAN VEGA Compact LMH (s5121) with an energy-dispersive X-ray (EDX) analyzer was used.

The granulometric composition was determined using a Horiba LA 950 laser particle size analyzer (Horiba, Japan) by the method of scattering and detection of reflected/refracted laser light. Chemical analysis was performed by atomic emission spectroscopy on a JY-48 inductively coupled plasma spectroanalyzer. The specific surface area of dust particles was estimated by the low-temperature nitrogen adsorption method (BET method) on a TriStar 3000 automatic analyzer (Micromeritics, USA).

To reduce the particle size of SBD and increase its reactivity, we grind it in a GEFEST-2 planetary-centrifugal mill. Zirconium oxide was used as the material for the drum lining and for the grinding balls with a diameter of 5 mm. Subsequent tableting was performed on a PGD-400 manual hydraulic press with a force of 7 tons (pressure 180 bar) in a mold with a diameter of 10 mm. Thereafter, the samples were sintered in a laboratory furnace under a vacuum of $3 \cdot 10^{-4}$ Pa with an overpressure of Ar of 151 kPa at a temperature of 750 ^{0}C with a holding time of 30 min. The hardness of the annealed samples was studied by the Vickers method on a PMT-3M microhardness tester with an applied load of 0.1 kg.

Materials and their characteristics

The production of V–Al master alloys is based on the exothermic reaction of aluminothermic reduction of metal oxides with a reductant according to the following reactions [12, 13]:

$$3V_2O_5 + 10Al \rightarrow 6V + 5Al_2O_3, \quad (1)$$

$$3V + Al \rightarrow V_3Al. \quad (2)$$

As a result, a dense ingot is obtained from the charge material in a lined crucible, with slag (Al_2O_3) located in the upper layer.

According to [14], the master alloy is the intermetallic compound V_3Al with a hexagonal structure. It is presented in the equilibrium phase diagram of the V–Al system [13]. To remove slag inclusions and oxide films from the ingot surface, automated cleaning is made in a shot-blasting unit. The abrasive material used is chilled cast steel shot with a particle size of 0.5–0.7 mm. At the shot-blasting cleaning stage, a large amount of disperse material accumulates in the dust collection filter – SBD.

Indeed, SBD is not involved in the subsequent (secondary) production cycle and is not processed. Due to the high cost of recycling, it is stored in the enterprise warehouses and considered as waste. According to plant analyses of elemental composition, the shot-blasting dust contains components based on vanadium, aluminum, and iron. The amount of waste generated reaches 500–1000 kg monthly.

Fig. 1 shows the morphology of shot-blasting dust from VnAl-65 (a) and VnAl-1 (b) master alloys.

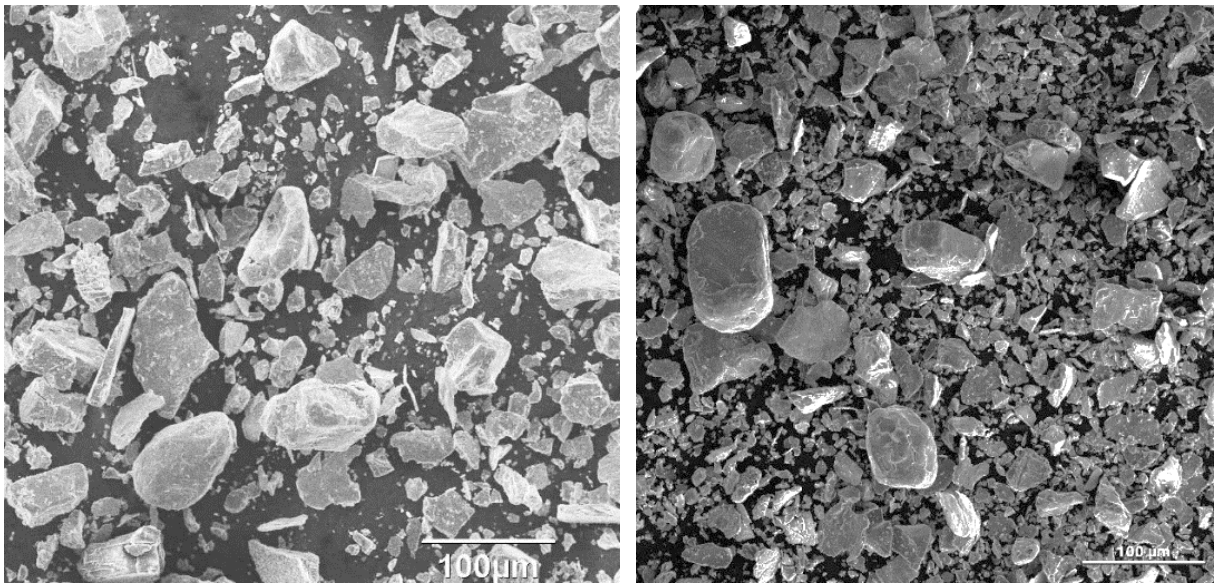

a *b*

Fig. 1. Micrographs of SBD from master alloys: a) VnAl-65; b) VnAl-1.

However, there are a lot of fine dust fractions and particles with sizes greater than several tens of micrometers. They have an irregular, fragmental shape with a developed rough surface. The large particles have a lamellar structure.

For a more detailed morphological analysis of the distribution of SBD components depending on their chemical composition and size, the industrial by-product was sieved through sieves (mesh size: 0.063 mm, 0.04 mm) with separation of particles into fractions: greater than 63 μm, from 40 to 63 μm, and less than 40 μm. Figs. 2 and 3 present the results of the sieve analysis of shot-blasting dust from both master alloys with EDX analysis.

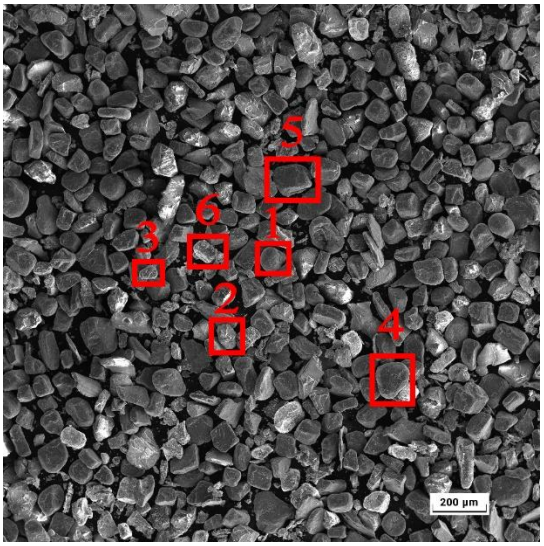

a

EDX analysis regions (mass %):
1) – 4.2 Al, 4.7 O, 1.9 V, 89.3 Fe;
2) – 49.8 Al, 47.5 O, 0.8 V, 2 Fe;
3) – 21.7 Al, 13.8 O, 61.9 V, 2.6 Fe;
4) – 16.7 Al, 10.3 O, 60.3 V, 12.7 Fe;
5) – 13.7 Al, 9.8 O, 72.9 V, 3.6 Fe;
6) – 18.2 Al, 18.7 O, 59.6 V, 3.5 Fe.

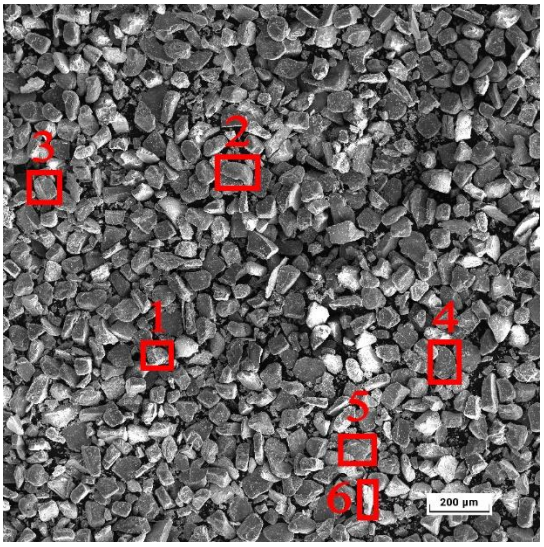

b

EDX analysis regions (mass %):
1) – 45.9 Al, 37.6 O, 3.1 V, 13.4 Fe;
2) – 5.2 Al, 4.9 O, 4.5 V, 85.4 Fe;
3) – 23 Al, 7.7 O, 65.8 V, 3.5 Fe;
4) – 26.1 Al, 7.3 O, 65.2 V, 1.4 Fe;
5) – 23.3 Al, 6.6 O, 65 V, 5.2 Fe;
6) – 6.3 Al, 5.5 O, 3.7 V, 84.5 Fe.

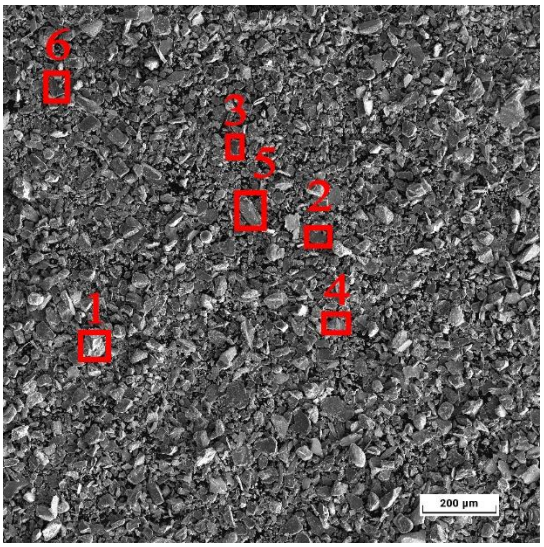

c

EDX analysis regions (mass %):
1) – 38.3 Al, 46.2 O, 11.8 V, 3.7 Fe;
2) – 1.1 Al, 0.7 O, 1.4 V, 96.8 Fe;
3) – 28.7 Al, 4.9 O, 64.1 V, 2.3 Fe;
4) – 2.6 Al, 1.8 O, 3.8 V, 91.8 Fe;
5) – 17.8 Al, 9.5 O, 68.4 V, 4.2 Fe;
6) – 18.4 Al, 9.2 O, 70.9 V, 1.5 Fe.

Fig. 2. Morphology and EDX analysis of shot-blasting dust particle fractions from VnAl-65 master alloy depending on the fraction: a) > 63 µm; b) 40–63 µm; c) < 40 µm.

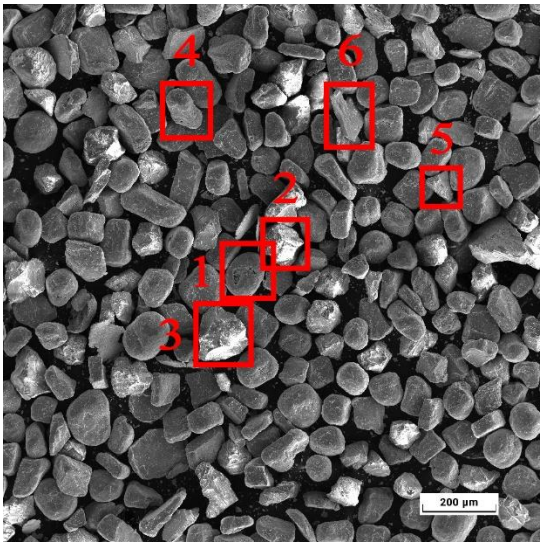

a

EDX analysis regions (mass %):
1) – 2.7 Al, 2.7 O, 4.1 V, 90.5 Fe;
2) – 49.4 Al, 47 O, 1.5 V, 2.1 Fe;
3) – 54.9 Al, 33.2 O, 1.6 V, 10.3 Fe;
4) – 15.5 Al, 16.3 O, 47.3 V, 20.9 Fe;
5) – 46.1 Al, 47.6 O, 2.0 V, 4.4 Fe;
6) – 20.7 Al, 25.3 O, 32.4 V, 21.6 Fe.

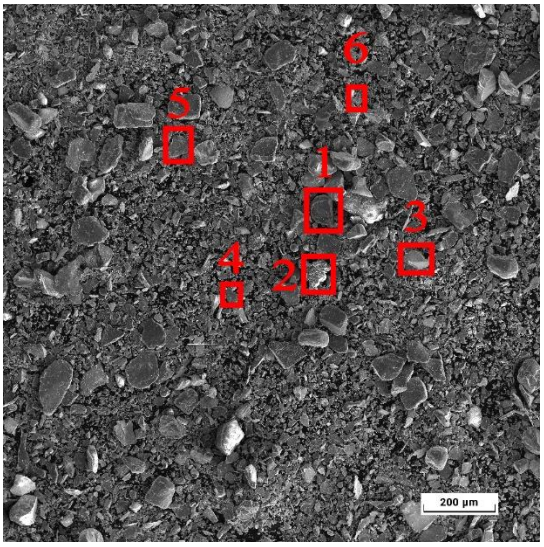

b

EDX analysis regions (mass %):
1) – 26.2 Al, 5.8 O, 65.2 V, 2.8 Fe;
2) – 47.4 Al, 41.5 O, 3.4 V, 7.6 Fe;
3) – 44.8 Al, 44 O, 3.7 V, 7.5 Fe;
4) – 3.7 Al, 5 O, 3.1 V, 88.1 Fe;
5) – 3.1 Al, 4.4 O, 3.7 V, 88.9 Fe;
6) – 49.5 Al, 42.5 O, 1.9 V, 6.1 Fe.

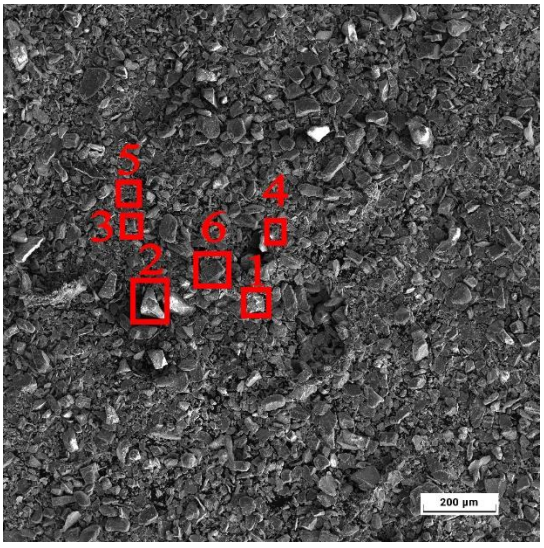

c

EDX analysis regions (mass %):
1) – 58.2 Al, 36.7 O, 2.2 V, 2.9 Fe;
2) – 56.1 Al, 42.5 O, 0.5 V, 0.9 Fe;
3) – 27.4 Al, 8.9 O, 59.1 V, 4.6 Fe;
4) – 46.7 Al, 44.8 O, 3.4 V, 5.2 Fe;
5) – 5.7 Al, 6.0 O, 4.2 V, 84.1 Fe;
6) – 6.7 Al, 9.2 O, 67.8 V, 16.3 Fe.

Fig. 3. Morphology and EDX analysis of shot-blasting dust particle fractions from VnAl-1 master alloy depending on the fraction: a) > 63 µm; b) 40–63 µm; c) < 40 µm.

According to X-ray phase analysis of SBD from VnAl-65 master alloy (Fig. 4a), it is a mechanical mixture of the composition: 50 wt. % Al_2O_3, 38 wt. % V_3Al, 8 wt. % Fe and 4 wt. % Fe_2O_3. VnAl-1 is in the following form: 47 wt. % Al_2O_3, 42 wt. % V_3Al, 8 wt.% Fe, and 3 wt.% Fe_2O_3 (Fig. 4b).

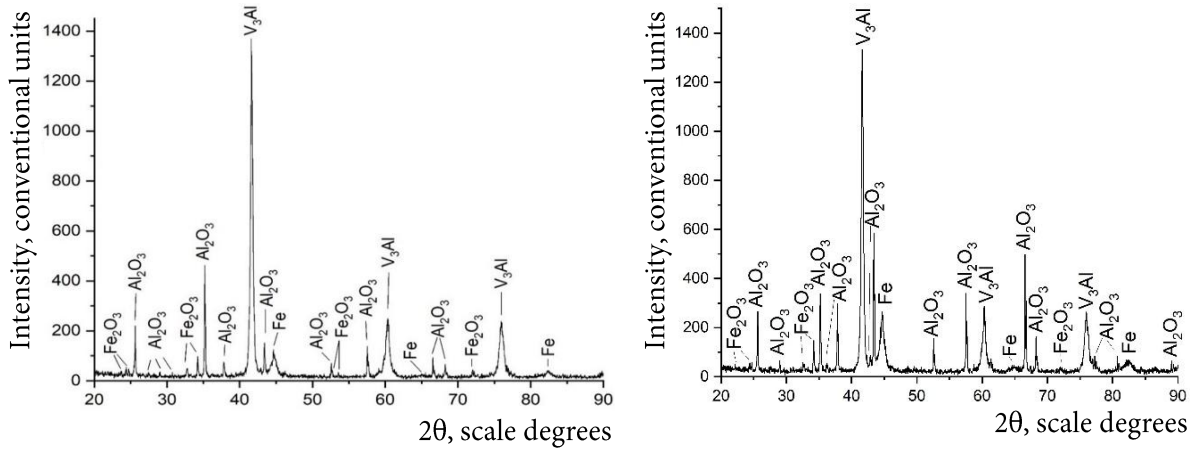

a *b*

Fig. 4. X-ray diffraction patterns of SBD from VnAl-65 (a) and VnAl-1 (b) master alloys.

Chemical analysis of SBD from VnAl-65 master alloy showed a content of V – 34.3 wt.%, Fe – 10.7 wt.%, O – 22.3 wt.%, Al – 32.2 wt.%, and accompanying impurities at the level of a few hundredths of a percent. In the case of VnAl-1: V – 38.5 wt.%, Fe – 10.1 wt.%, Al – 31.1 wt.%, O – 19.8 wt.%, and other impurities are in similar amounts.

By analogy with the study of particle morphology using an electron microscope depending on the particle fraction (Figs. 2, 3), X-ray phase analysis of the phase distribution in the composition of SBD from VnAl-65 and VnAl-1 master alloys after sieving was performed (Table 1).

Table 1. Fractional and X-ray phase composition before and after sieving.

SBD fraction size, μm	Content of fractions after sieving, %	V_3Al, wt.%	Al_2O_3, wt.%	Fe, wt.%	Fe_2O_3, wt.%
VnAl-65					
Initial	100	38	50	8	4
< 40	71.4	32	63	3	2
40 - 63	10.2	28	66	4	2
> 63	18.4	25	67	6	2
VnAl-1					
Initial	100	42	47	8	3
< 40	72.1	36	60	3	1
40 - 63	11.6	32	63	4	1
> 63	16.3	29	64	6	1

According to Table 1 and Figs. 2 and 3, the main content in $SBD_{VnAl-65}$ consists of particles with a fraction size of < 40 μm, accounting for 71.4%, with larger particles (> 63 μm) present in an amount of 18.4%. X-ray phase analysis showed an increase in the Al_2O_3 component with increasing particle size by approximately 25%. It is accompanied by a simultaneous decrease in the amount of the intermetallic compound V_3Al. In the case of SBD_{VnAl-1}, a similar trend is observed. Predominantly, this mixture contains about 72.1% of particles with a size < 40 μm,

and 16.3% of larger particles (> 63 μm). The amount of Al_2O_3 also increases with increasing particle size while the V_3Al content decreases.

Experimental results

To reduce the particle size and increase their reactivity, SBD from VnAl-1 and VnAl-65 master alloys was subjected to grinding in a planetary-centrifugal mill. The grinding was at a speed of 1300 rpm in four time modes: 10, 30, 60, and 120 min. The average particle size of the initial shot-blasting dust from each of the master alloys was about 16 μm. Table 2 presents the results of studying the effect of grinding duration on the average particle size using the example of shot-blasting dust from VnAl-1 master alloy.

Table 2. Effect of mechanical activation time on the average particle size of SBD_{VnAl-1}.

Grinding time, min.	Average particle size, μm
0	16.0
10	10.0
30	9.5
60	7.8
120	10.0

According to Table 2, the grinding efficiency of SBD_{VnAl-1} samples is achieved at a processing time of 60 min. In this case, the average particle size reaches a level of about 7.8 μm, with an increase in specific surface area by almost 6.5 times ($S_{sp.0}$ – 0.2925; $S_{sp.60}$ – 1.9048). Increasing the processing time to 120 min leads to the opposite effect – an increase in the average size to about 10.0 μm due to particle agglomeration. In the case of SBD from VnAl-65 master alloy, a similar pattern is observed. The optimal grinding time was 60 min; the average particle size reached 8 μm with a change in specific surface area from 0.3561 to 1.8834 m^2/g.

According to X-ray phase analysis, during the mechanochemical activation, a change in the content of components in the SBD_{VnAl-1} mixture occurs. However, before grinding, as noted in Fig. 4b they were as follows: Al_2O_3 - 47 wt.%, V_3Al - 42 wt.%, Fe - 8 wt.%, Fe_2O_3 - 3 wt.%; after grinding they were as follows: Al_2O_3 - 32 wt.%, V_3Al - 52 wt.%, Fe - 10 wt.%, Fe_2O_3 - 6 wt.%. As a result, Al_2O_3 content decreased by more than 30%. This is explained by the fact that under high-energy impact, a thin layer of amorphous aluminum oxide is formed on the particle surface, i.e., a process of Al_2O_3 amorphization occurs [5; 15]. Simultaneously, the diffraction pattern shows an increase in the intensity of peaks from Fe_2O_3, Fe, and the intermetallic compound V_3Al. For $SBD_{VnAl-65}$ a similar trend is observed. Indeed, before grinding (Fig. 4a) the phase composition was as follows: Al_2O_3 - 50 wt.%, V_3Al - 38 wt.%, Fe - 8 wt.%, Fe_2O_3 - 4 wt.%; after grinding: Al_2O_3 - 35 wt.%, V_3Al - 46 wt.%, Fe - 12 wt.%, Fe_2O_3 - 7 wt.%.

The next step was the synthesis of the composite material. For this purpose, mixtures were prepared containing 5% SBD_{VnAl-1} (before and after grinding) and 95% Al in the form of APZh grade powder. Aluminum powder of the APZh grade has a spherical and tear-drop shape with a smooth surface, characteristic of powders obtained by inert gas atomization. The average particle size of the powder is about 52.5 μm; a specific surface area of 0.19 m^2/g. These compositions were pressed into tablets with a diameter of 10 mm, a thickness is 6 mm, and a mass is 2 g; sintered in a vacuum furnace at 750 °C in argon with a holding time of 30 min. X-ray phase analysis of the sintered samples showed that the material obtained from unmilled

SBD_{VnAl-1} consists of 88 wt.% Al, 9 wt.% $Al_{23}V_4$, 2 wt.% Al_3V and 1 wt.% Fe_4Al_{13}. The sample with milled SBD_{VnAl-1} affected the amount of identified phases: 85 wt.% Al, 10 wt.% $Al_{23}V_4$, 3 wt.% Al_3V and 2 wt.% Fe_4Al_{13}. In both cases, no crystalline oxide phases were detected.

The synthesis of the composite material is under similar conditions from mixtures of APZh and VnAl-65 (before and after grinding). XRD analysis showed results similar to those for the Al + SBD_{VnAl-1} samples, differing only slightly in quantitative terms: without grinding – 89 wt.% Al, 8 wt.% $Al_{23}V_4$, 1 wt.% Al_3V and 2 wt.% Fe_4Al_{13}; after grinding - 87 wt.% Al, 9 wt.% $Al_{23}V_4$, 2 wt.% Al_3V and 2 wt.% Fe_4Al_{13}. Thus, the introduction of SBD after grinding affects the reduction of Al and Al_3V content and the increase in the amounts of $Al_{23}V_4$ and Fe_4Al_{13} in the composite. It indicates an increase in the reactivity of the shot-blasting dust due to mechanical activation.

The absence of Fe_2O_3 in the structure of the sintered samples is explained by the fact that during synthesis, a thermite reaction occurs between liquid aluminum and iron oxide [16]:

$$2Al + Fe_2O_3 \rightarrow 2Fe + Al_2O_3, \quad (3)$$

$$4Fe + 13Al \rightarrow Fe_4Al_{13}. \quad (4)$$

Metallic iron, having reacted with liquid aluminum, forms an intermetallic compound of composition Fe_4Al_{13} [17, 18]. It is in good agreement with the general principles of processing iron-containing waste from non-ferrous metallurgy. As noted in the review [18], combined pyro-hydrometallurgical methods allow efficient extraction of iron from slags and its conversion into valuable compounds. In our study, the thermite reaction (3) and the subsequent interaction of iron with aluminum (4) demonstrate the implementation of a similar approach in solid-phase synthesis. It agrees with the work of [19]. Also, the grinding of SBD noticeably affected the phase formation processes of the composites: the transition at 750 °C of the intermetallic compound V_3Al (peritectic $T_{formation}$ 1360 °C) into $Al_{23}V_4$ ($T_{peritectic\ formation}$ 736 °C), i.e., a dissolution process of V_3Al in Al took place. The interaction at the phase boundaries (V_3Al / Fe_2O_3 / Al_2O_3 /Al) contributes to the formation of a heterogeneous structure of the material.

Fig. 5 shows micrographs of the surface of the composites Al + SBD_{VnAl-1} (a) and Al + $SBD_{VnAl-65}$ (b) after processing.

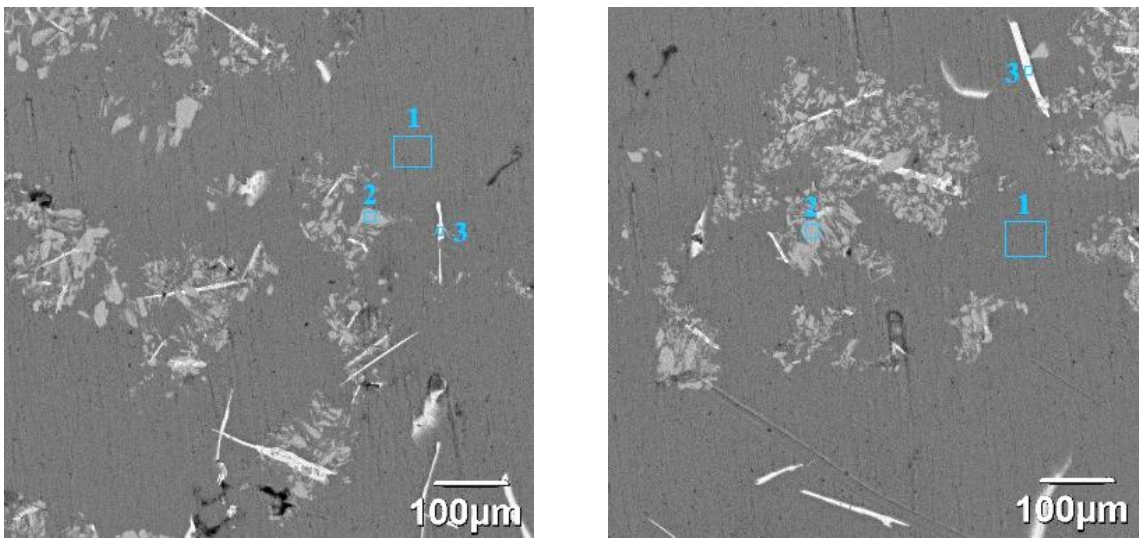

a *b*

Fig. 5. Microstructure of composites after using SBD subjected to grinding: a) Al + SBD_{VnAl-1}; b) Al + $SBD_{VnAl-65}$.

In the aluminum matrix, the intermetallic compounds are uniformly distributed in the field of the polished section. EDX analysis for the Al + SBD_{VnAl-1} sample showed (Fig. 5a) that area 1 corresponds to aluminum, area 2 contains 75.3 wt.% Al and 24.7 wt.% V, and area 3 contains 70.1 wt.% Al and 29.9 wt.% Fe. Over the entire plane of the polished section of the Al + SBD_{VnAl-1} composite, chemical analysis showed the following elemental content: 92.2 wt.% Al, 5.9 wt.% V, and 1.9 wt.% Fe. For Al + $SBD_{VnAl-65}$ (Fig. 5b): area 1 is the aluminum matrix, area 2 contains 78.4 wt.% Al and 21.6 wt.% V, and area 3 contains 73.5 wt.% Al and 26.5 wt.% Fe. According to EDX analysis of the entire plane of the polished section of Al + $SBD_{VnAl-65}$: 94.1 wt.% Al, 4.3 wt.% V, and 1.6 wt.% Fe. Averaged point analysis of both samples showed that in the zone of the aluminum matrix located between vanadium intermetallics, the V content is about 0.9 at.%. According to the V–Al phase diagram [13], the solubility of vanadium in aluminum at temperatures of 735, 660, and 500 °C is 0.91, 0.2, and 0.11 at.%, respectively. It is consistent with the result obtained above.

Table 3 presents the results of microhardness measurements of the synthesized Al + SBD composites depending on the type of master alloy and mechanical activation time, in comparison with the material from the original APZh grade aluminum.

Table 3. Microhardness of sintered samples.

Sample	Average microhardness value, $HV_{0.1}$
APZh	48.3
Al+SBD_{VnAl-1} without grinding	65.3
Al+SBD_{VnAl-1} after grinding	67.2
Al+$SBD_{VnAl-65}$ without grinding	58.7
Al+$SBD_{VnAl-65}$ after grinding	60.2

According to Table 2 and Fig. 5, the introduction of 5% disperse industrial by-product into the aluminum powder leads to significant strengthening of the matrix during sintering due to the absence of crystalline oxide components in the final product, the appearance of intermetallic compounds during the thermite reaction of Al–Fe_2O_3, and the formation of refractory vanadium compounds (V_3Al + Al → Al_3V, Al_3V + Al → $Al_{23}V_4$). The obtained composite materials demonstrate a homogeneous microstructure with a uniform distribution of strengthening phases. Indeed, the hardness values depend on the initial composition of the SBD and the mechanical activation time.

Conclusions

1. The certification of shot-blasting dusts from VnAl-1 and VnAl-65 master alloys has been conducted. These dusts represent a complex mechanical mixture consisting of the intermetallic compound V_3Al, aluminum oxide (Al_2O_3), metallic iron, and its oxide (Fe_2O_3). The bulk of the particles (~70%) has a size of less than 40 μm. Indeed, with increasing particle size of SBD, the Al_2O_3 content increases and the V_3Al content decreases.

2. Treatment in a planetary mill effectively influences the dispersity of dust particles. The optimal grinding time (60 min) has been established. During this time the partial amorphization of Al_2O_3 occurs and the average particle size decreases from 16 to about 8 μm

with an increase in specific surface area by several times. It contributes to an improvement in the reactivity of the mixture during the synthesis of composite materials.

3. During sintering, a thermite reaction between aluminum and iron oxide proceeds, along with partial dissolution of Al_3V in the aluminum matrix. The presence in the structure of the final material of the intermetallic compounds Al_3V, $Al_{23}V_4$ and Fe_4Al_{13} without crystalline oxide components contributes to significant strengthening of the synthesized composites.

4. The obtained composites are close in hardness to well-known widely used aluminum alloys: avial AD35 ($HV_{0.1}$ = 68.5), silumins Al4, Al9 ($HV_{0.1}$(Al4) = 53-73.7, $HV_{0.1}$(Al9) = 47-53).

Funding:

The present work was performed in accordance with a state order to the Institute of Solid State Chemistry, Ural Branch, Russian Academy of Sciences, № 124020600007-8.

Conflict of interest:

The authors declare no conflict of interest in financial or any other sphere.

References

1. Master alloys based on refractory rare metals for vanadium-based titanium alloys. TU 1761-022-25087982-98 (with amendments 1–4), JSC Uralredmet: Yekaterinburg (in Russian).
2. **Nikitin K.V.** Recycling of aluminum-based metal waste. Samara: SamSTU, 2016. 34 p. (in Russian).
3. **Omran A.M.** Fabrication and characterization of Al-based in situ composites reinforced by Al_3V intermetallic compounds. *E3 J. Sci. Res.* 2014, 2(**2**), 26-34.
4. **Blinichev V.N., Bobkov S.P., Gayumdzhan P.P.** Influence of the design of mills on specific energy consumption and mechanochemical transformations of ground materials. Reports of the VII All-Union Symposium on Mechanoemission and Mechanochemistry of Solids. Part 1. Tashkent, 1981. pp. 73–78. (in Russian).
5. **Avvakumov E.G.** Mechanical methods for activation of chemical processes. Novosibirsk: Nauka, 1986, 305 p. (in Russian).
6. **S.V. Zhukov, M.P. Nikitin, A.K. Petrov;** Pat. RF 2793561, 2023. (in Russian).
7. **Boldyrev V.V., Abakumov E.G., Logvienko A.T.** Efficiency of grinding apparatus for mechanical activation of solids. Mineral Processing. Novosibirsk: Nauka, 1977. pp. 3–10. (in Russian).
8. **Gerold E., Luznik L, Samberger S., Antrekowitsch H.** Sustainable extraction and recycling of non-ferrous metals: a review from a European perspective. *Pholos. Trans. A Math. Phys. Eng. Sci.* 2024, 382, 20240173. https://doi.org/10.1098/rsta.2024.0173
9. **Krupnov L.V., Midyukov D.O., Datsiev M.S., Ilyin V.B.** Changes in the resource base of heavy non-ferrous metal production using the example of copper and nickel. *Gornyi Zhurnal.* 2024, (**3**), 10-16. doi.org/10.17580/gzh.2024.03.01 (in Russian).
10. **Baklanov M.N., Eselevich D.A., Shevchenko V.G.** Physicochemical investigation of the feasibility of using waste from shot-blasting cleaning of Al–V master alloys for obtaining functional materials based on aluminum. *Rasplavy.* 2022, (**1**), 3-11. https://doi.org/10.31857/S0235010622010029 (in Russian).
11. **Rietveld H.M.** A profile refinement method for nuclear and magnetic structures. *J. Appl. Crystallogr.* 1969, 2(**2**), 65-71.
12. **Lyakishev N.P., Pliner Yu.L., Ignatenko G.F., Lappo S.I.** Aluminothermy. Moscow: Metallurgiya, 1978, 424 p. (in Russian).
13. **Lyakishev N.P.** Phase diagrams of binary metallic systems: Handbook: In 3 vols.: Vol. 1. Edited by N.P. Lyakishev. Moscow: Mashinostroenie, 1996, 992 p. (in Russian).

14. **Chumarev V.M., Marevich V.P., Chentsov V.P., Pazdnikov I.L., Pankov I.A., Baklanov M.N.** Phase composition and melting temperatures of aluminothermic master alloys of refractory rare metals. *Rasplavy*. 2009, (**3**), 29-35 (in Russian).
15. **Gutman E.M.** Mechanochemistry of metals and corrosion protection. Moscow: Metallurgiya, 1974, 232 p. (in Russian).
16. **Plantier K.B., Pantoya M.L., Gach A.E.** Combustion wave speeds of nanocomposite Al/Fe_2O_3: the effects of Fe_2O_3 particle synthesis technique. *Combust. Flame.* 2005, 140(**4**), 299-309. DOI: https://doi.org/10.1016/j.combustflame.2004.10.009
17. **Black P.J.** The Structure of $FeAl_3$. *Acta Crystallogr.* 1955, 8, 43. https://doi.org/10.1107/S0365110X5500011X
18. **Han K., Ohnuma I., Kainuma R.** Experimental determination of phase equilibria of Al-rich portion in the Al-Fe binary system. *J. Alloys Compd.* 2016, 668, 97-106. https://doi.org/10.1016/j.jallcom.2016.01.215
19. **Qin Z., Xiao J., Du T., Cheng R., Zhang J.** Resource utilization strategy of Fe-bearing smelting slag in China: a review. *Miner. Eng.* 2024, 219, 109066. https://doi.org/10.1016/j.mineng.2024.109066

Received 20.03.2026
Approved after reviewing 15.04.2026
Accepted 04.05.2026